Exciton-polariton in WS_2 microcavity in the presence of the optical Stark effect

Mahnoor Shahzadi[1], Weili Zhang (张伟利)[1,*], and M. T. Khan[2]

[1]*School of Information and Communication Engineering, University of Electronic Science and Technology of China, Chengdu 611731, China*

[2]*Electrical Engineering Department, University of Lahore, Islamabad Campus 54000, Pakistan*

**Corresponding author: wl_zhang@uestc.edu.cn*

Received December 12, 2018; accepted January 10, 2019; posted online February 1, 2019

Exciton-polaritons offer an exceptional platform for future photoelectronic and quantum information applications. The influence of the optical Stark effect on exciton-polaritons in a microcavity embodied with a monolayer WS_2 is studied. A polarization dependent model is proposed to study the change of strongly coupled excitons and photons in a WS_2 microcavity. It is revealed through both steady and dynamical states analysis that an outside optical Stark pulse can effectively vary the polariton characteristics, such as dispersion, exciton, and photon fractions, through blue shifting of excitonic resonance. Thus, the analysis and control of exciton-polaritons in a WS_2 microcavity via a spin-selective trigger could be achievable.

OCIS codes: 240.5420, 260.6580, 160.2100.

doi: 10.3788/COL201917.020014.

Polaritons are half-matter half-light quasi-particles that are formed in semiconductors when excitons are strongly coupled with light. In optoelectronics, exciton-polaritons have gained noteworthy attention for their distinctive features. The literature shows that the photonic component of these quasi-particles makes them lighter in mass so they can be manipulated and fall to Bose–Einstein condensation easier (i.e., used to generate low-threshold lasers and superfluid), and the excitonic component produces strong nonlinearities that are important for the implementations of various polaritonic operations, such as optical bistability, solitons, vortex, switching, and logical controls[1–8].

Transition metal dichalcogenides (TMDs) and the addition of phosphorene and MXene to the two-dimensional (2D) family allow for a thorough understanding of the interaction of light with the atomically thin materials in the determination of the feasibility in photonic applications[9–15]. Due to their fantastic excitonic characteristics, such as large binding energy, time reversal symmetry in the Brillouin zone, quantum effects, valley degree of freedom, and multifold-controllable energy level, room temperature polaritons have been obtained based on various 2D materials[10,15]. However, the characteristics of polaritons in the presence of an outside field (electronic or magnetic) are still an open question that requires further exploration.

The characteristic of excitons subjected to the optical Stark (OS) effect is studied. As mentioned in literature[11], the OS effect is a coherent light–matter interaction describing the modification of quantum states by nonresonant light illumination in atoms, solids, and nanostructures. It is a method of splitting and shifting the energy of particles by means of an external optical source[16,17]. When the OS field is applied to the TMD layer, it will cause a blue shift of the exciton energy. As the OS field does not cause a population increase of the exciton reservoir, it causes the energy shift in a fast transient, which paves the way for ultrafast manipulation of polaritons[18,19]. Additionally, the spin-selective characteristics of the OS effect provide additional degrees of freedom to control polaritons[3,8]. All of these are useful in future applications of optical information, such as switching, spacial shaping of potential energy, and spintronic applications[20].

Recently, the OS effect in 2D monolayer WS_2 is studied at room temperature[11,21,22]. The study only focused on bare excitons without strong coupling with cavity photons. This work will investigate the influence of the OS effect on strongly coupled excitons and photons, the so-called polaritons. The fundamental way in such a work is to introduce an OS pulse to stimulate the energy shift of both upper polariton (UP) and lower polariton (LP) branches (i.e., blue shift). A polarization-sensitive exciton-polariton coupling model is used to study the dispersion as well as the dynamical characteristics of the polaritons in the presence of the OS effect. Based on this model, steady state and transient analyses are performed to reveal the influence of the OS effect on the excitonic and photonic components of the polaritons.

For theoretical study, the general Gross–Pitaevskii equation is utilized to describe strong coupling of excitons and photons[19,23–26]. The effective mass of photons is quite smaller than that of the excitons. Thus, in the equation, only the dispersion of the photons needs to be considered. It states as $\omega_x = \omega_x^0 + \frac{\hbar^2\nabla^2}{2m_c}$, where ω_x^0 is the cavity mode energy for $k = 0$ (k is the in-plane wave vector), m_c is the effective mass of photons, and ∇^2 is the Laplace

operator. The exciton energy is given as $\omega_x = \omega_x^0 + \delta$ with ω_x^0 the free-running exciton energy and δ the OS effect inducted energy shift of the exciton. δ is proportional to the intensity of the OS pulse (i.e., $|E_0|$) and inversely proportional to energy detuning (i.e., Δ) between the OS photon and the exciton. Thus, $\omega_x = \omega_x^0 \frac{M_{ab}|E_0|^2}{2\Delta}$, where M_{ab} is the dipole moment matrix[10]. Here, the spin-sensitive excitation of the OS effect is added to the model through the dipole moment matrix $M_{ab}^{\pm} = M_{ab}\begin{bmatrix}1 & 0\\ 0 & 1\end{bmatrix}\begin{bmatrix}\sigma^+\\ \sigma^-\end{bmatrix}$, where $\pm$ denotes the spin-up and spin-down states, and σ is the unit vector of the spin state. It is clear from this relation that the energy shift of excitons in the two valley spin states is only induced by the OS pulse of corresponding circular polarization. If the spin-sensitive case is considered, the Gross–Pitaevskii model is extended as given below:

$$i\hbar\frac{\partial}{\partial t}\begin{pmatrix}\psi_c^+\\ \psi_x^+\\ \psi_c^-\\ \psi_x^-\end{pmatrix} = \begin{pmatrix}E_{\text{in}}^+\\ 0\\ E_{\text{in}}^-\\ 0\end{pmatrix} + (H_0 + M)\times\begin{pmatrix}\psi_c^+\\ \psi_x^+\\ \psi_c^-\\ \psi_x^-\end{pmatrix}, \quad (1)$$

where the Hamiltonian H_0 reads

$$H_0 = \begin{pmatrix}\omega_c^0(k) & \frac{\Omega_R}{2} & 0 & 0\\ \frac{\Omega_R}{2} & \omega_x^0 + \frac{M_{ab}^+|E_0^+|^2}{2\Delta} & 0 & 0\\ 0 & 0 & \omega_c^0(k) & \frac{\Omega_R}{2}\\ 0 & 0 & \frac{\Omega_R}{2} & \omega_x^0 + \frac{M_{ab}^-|E_0^-|^2}{2\Delta}\end{pmatrix},$$

and the matrix M reads

$$M = \begin{pmatrix}-i\hbar\frac{\gamma_c}{2} & 0 & 0 & 0\\ 0 & g_1|\psi_x^+|^2 + g_2|\psi_x^-|^2 - i\hbar\frac{\gamma_x}{2} & 0 & 0\\ 0 & 0 & -i\hbar\frac{\gamma_c}{2} & 0\\ 0 & 0 & 0 & g_1|\psi_x^-|^2 + g_2|\psi_x^+|^2 - i\hbar\frac{\gamma_x}{2}\end{pmatrix}.$$

Ω_R is the Rabi frequency, γ_c and γ_x are the decay rate of the photon and exciton, respectively, and g_1 and g_2 denote the nonlinear parameters of co-polarized and cross-polarized states.

For the static analysis, a homogenous cavity structure is supposed, and the loss and nonlinear terms are neglected, i.e., $E(x,t) = \gamma_{c,x} = g_{1,2} = 0$. The two eigenstates of the UP and LP branches E_{UP} and E_{LP} with the influence of the OS effect are given as

$$E_{\text{UP,LP}}^{\pm} = \frac{1}{2}\left[\omega_c^0(k) + \left(\omega_x^0 + \frac{M_{ab}^{\pm}|E_0^{\pm}|^2}{2\Delta}\right)\right] \pm \frac{1}{2}\sqrt{\left[\omega_c^0(k) - \omega_x^0 - \frac{M_{ab}^{\pm}|E_0^{\pm}|^2}{2\Delta}\right]^2 + \Omega_R^2}. \quad (2)$$

For numerical study, typical values of the parameters are listed in Table 1.

Table 1. Specific Symbols and Values

Symbol	Parameter	Value
$g_{1,2}$	Nonlinear parameter	0
γ_c	Decay rate of the photon	0
γ_x	Decay rate of the exciton	0
ω_c^0	Cavity mode energy	2 eV
Ω_R	Rabi frequency	70 meV
Δ	Energy detuning	0.2 meV
m_c	Mass of photon	$10^{-5}m_x$
m_x	Mass of exciton	5.11×10^5 eV · c^2 · S^2/m^2
E_g	Quasi-particle bandgap	2.3 eV

The parameter $M_{ab} = \sqrt{\left(\frac{eh}{\omega_x^0}\right)^2\frac{E_g}{2m_x}}$, where e is the electron charge, E_g is the quasi-particle band gap, and m_x is the effective mass of the conduction electron[11]. In fact, this parameter reflects the influence of material characteristics on the OS effect. In the proposed case, it is calculated to be 1.159×10^{-9}. Once this parameter is determined, there is a change of polariton dispersion for different values of $\frac{E^2}{\Delta}$, as given in Fig. 1.

It can be seen from the curves, as depicted in Fig. 1a, that the Stark effect is causing a blue shift of the exciton energy, e.g., the shift of exciton energy δ increases linearly as a function of $\frac{E^2}{\Delta}$, as in Fig. 1a. The dispersion curves in Fig. 1b indicate that the LP and UP branches also shift to a higher energy level and change their shapes. Moreover, the group velocity (i.e., slope efficiency of the dispersion curve) of the LP/UP branch increases or decreases, respectively. Thus, one can control the dispersion characteristics of polaritons through the OS effect. It is observed that if the value of Δ is 0.2 meV, an OS pulse with an amplitude in the order of megavolts (MV) is needed to shift the polaritonic at the milli electron volts (meV) scale. The energy shift of the UP and LP branches for different values of E_0 is shown directly in Fig. 1c. It is seen that the energy shift of the UP branch is larger than that of the LP branch for small values of k, and the case is the reverse for large values of k.

As polaritons are a mixture of photons and excitons, therefore, in a strong coupling regime, the Hopfield index of the photons as $C(k)$ and excitons as $X(k)$ satisfy the relation $|C(k)|^2 + |X(k)|^2 = 1$. In Fig. 1d, the values of

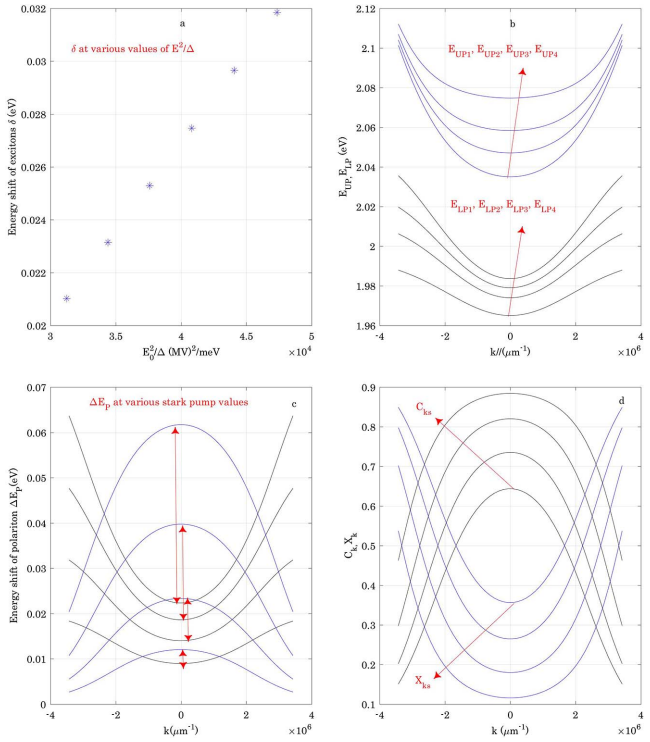

Fig. 1. Exciton energy and dispersion of polaritons for different values of an OS pulse. a, Energy shift of excitons as a function of $\frac{E^2}{\Delta}$. b, Dispersion of polaritons. c, Shift of the polariton dispersion. d, Changes of the excitonic and photonic fraction. In b–d, $\Delta = 0.2$ meV, and E_0 is 75, 100, 125, 150 MV, respectively (from down to up or from inside to outside).

C and X are provided as functions of k. It is observed that the anti-crossing point between $C(k)$ and $X(k)$ increases to a larger value of k and causes LPs/UPs and more photons/excitons when energy of the OS pump increases.

The energy shift of the LP and UP branches as a function of $\frac{E^2}{\Delta}$ is shown in Fig. 2. In contrast to the linear shift of exciton energy, the polariton branches shift exponentially and become more divergent when $\frac{E^2}{\Delta}$ increases.

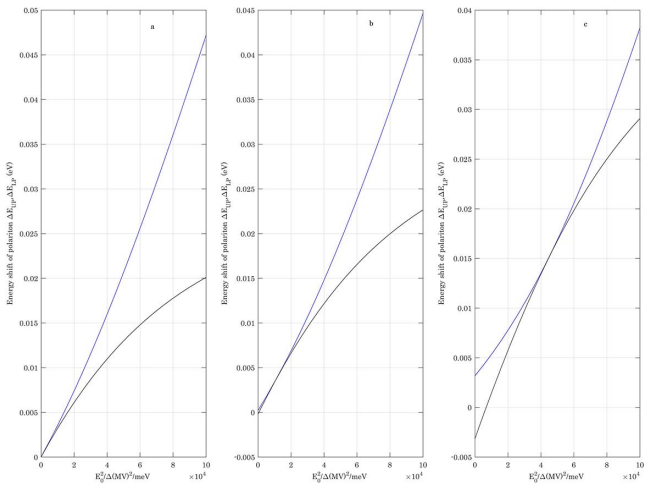

Fig. 2. Difference between UP and LP branches at various values of k, i.e., at $k = 0, 1, 2$ (a, b, and c, respectively).

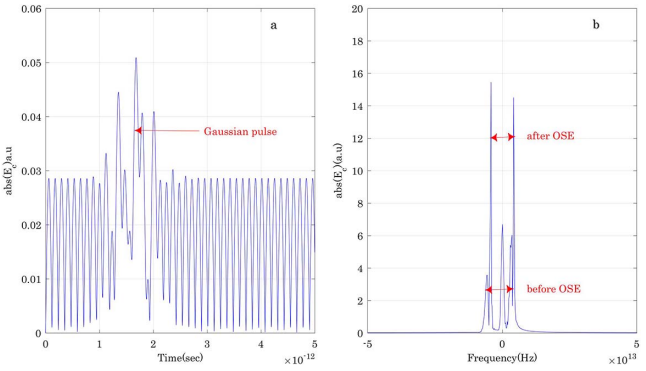

Fig. 3. Dynamic analysis of the Stark effect on the energy shift of the polaritonic field. a, Waveform in the time domain. b, Fast Fourier transform of the waveform. In the calculation, $k = 0$, $t_0 = 500$, and $a = 0.5$ ps.

The anti-crossing point of the two curves also increases with an increase in value of $\frac{E^2}{\Delta}$.

As the OS effect happens in a fast transient, the dynamical evolution of a polariton is also studied in Fig. 3 by utilizing the photonic fraction as an example. In such a case, Eq. (1) is solved numerically through the fourth-order Runge–Kutta (RK) method, and a transient OS pulse is applied with the form $E = Ae^{\left(-\frac{t-t_0}{a}\right)^2}$. In the proposed analysis, the values $t_0 = 500$ and $a = 0.5$ ps are taken. In Fig. 3a, fluctuation of the photonic waveform corresponds to the Rabi oscillation between the photons and excitons. When the OS pulse arrives, an envelope of the waveform exhibits a peak at the transient. The fast Fourier transform of the waveform exhibits a bifurcation (caused by the OS effect) for both the UP and LP branches. The Rabi splitting between the UP and LP branches is found to be 68 meV, which is approximate to the Rabi splitting of the proposed experimental value of 70 meV.

Furthermore, the spin-sensitive OS effect is analyzed in the consequent plots. It consists of right circularly polarized (RCP) and left circularly polarized (LCP) fields E_c^+ and E_c^-, related to two spins of the excitons. Firstly, it is supposed that the two polarization directions are equally pumped (i.e., $E_{\text{in}}^+ = E_{\text{in}}^- = E_{\text{in}}$) initially, while the OS pulse is in the RCP direction. In this case, the OS effect only influences the RCP component of the polaritons. The polarization degree is calculated as

$$\rho_{\text{out}} = \frac{|E_c^+|^2 - |E_c^-|^2}{|E_c^+|^2 + |E_c^-|^2}. \tag{3}$$

When there is no OS effect, $\rho_{\text{out}} = 0$, and ρ_{out} decreases with $\frac{E^2}{\Delta}$ increasing. Thus, polarization of the polaritons can also be adjusted through the spin-sensitive OS effect, as depicted in Fig. 4.

For experimental study, we can practically realize our work by sandwiching the monolayer of WS_2 between the two distributed Bragg reflectors. The sample consists of monolayers of WS_2 that can be grown by chemical

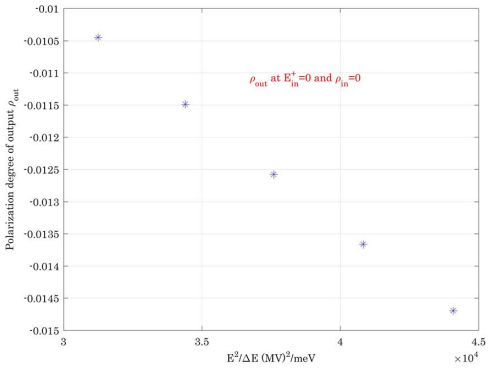

Fig. 4. Polarization degree versus $\frac{E^2}{\Delta}$ (simulation $E_{\text{in}} = 0.5$ is considered).

vapor deposition (CVD), and all optical measurements in this study are conducted at room temperature (300 K), similar to Refs. [10,11]. The role of a semiconductor microcavity (i.e., providing high Q cavity modes) and monolayer WS_2 is to provide well confined photons and excitons, respectively, that are necessary to realize strong coupling.

When multi-layer WS_2 is used, the energy of excitons will be changed, it might turn into an indirect band gap, and the non-linear effect needs to be considered, which we will leave for our future work. Besides, phosphorene and MXene also show direct bandgap and large exciton binding energy, which are favored to form polaritons. Here, we take WS_2 as a typical example of TMD in this study, as it shares the most common characteristics, like large binding energy of exciton and valley degree of freedom, and the known experimental parameters needed for our study.

The impact of the OS effect in a strongly coupled model of an exciton-polariton in a monolayer WS_2 microcavity has been perceived. A spin dependent mathematical model of the OS effect has been developed, and the accuracy of this spin controlled model is investigated. The proposed model proves that an outside polarized OS pulse can control the strongly coupled exciton-polariton dispersion and fraction ratios, both in time dependent and time independent analysis. This work paves a way to control the valley degree of freedom in a new manner. The potential applications of this model could be designing 2D material-based devices (switches, gates) to be controlled by an OS pulse, thus paving a way for optically controlled 2D material devices.

This work was supported by the National Natural Science Foundation of China (NSFC) (Nos. 61811530062 and 61575040) and the Sichuan Science and Technology Program (No. 2018HH0148).

References

1. T. Gao, P. S. Eldridge, T. C. H. Liew, S. I. Tsintzos, G. Stavrinidis, G. Deligeorgis, Z. Hatzopoulos, and P. G. Savvidis, Phys. Rev. B **85**, 235102 (2012).
2. D. Ballarini, M. De Giorgi, E. Cancellieri, R. Houdré, E. Giacobino, R. Cingolani, A. Bramati, G. Gigli, and D. Sanvitto, Nat. Commun. **4**, 1778 (2013).
3. W. L. Zhang and S. F. Yu, Opt. Express **18**, 21219 (2010).
4. Z. J. Yang, W. L. Zhang, R. Ma, X. Dong, S. L. Hanson, X. F. Li, and Y. J. Rao, Photon. Res. **5**, 557 (2017).
5. A. A. Raheli, H. R. Hamedi, and M. Sahrai, Laser Phys. **26**, 025201 (2015).
6. G. Lerario, A. Fieramosca, F. Barachati, D. Ballarini, K. S. Daskalakis, L. Dominici, M. De Giorgi, S. A. Maier, G. Gigli, S. Kéna-Cohen, and D. Sanvitto, Nat. Phys. **13**, 837 (2017).
7. H. Deng, H. Haug, and Y. Yamamoto, Rev. Mod. Phys. **82**, 1489 (2010).
8. D. Sanvitto and S. Kéna-Cohen, Nat. Mater. **15**, 1061 (2016).
9. J. S. Ponraj, Z. Q. Xu, and S. C. Dhanabalan, Nanotechnology **27**, 462001 (2016).
10. S. C. Dhanabalan, J. S. Ponraj, H. Zhang, and Q. Bao, Nanoscale **8**, 6410 (2016).
11. E. J. Sie, J. W. McIver, Y.-H. Lee, L. Fu, J. Kong, and N. Gedik, Proc. SPIE **9835**, 983518 (2016).
12. K. S. Novoselov, A. Mishchenko, A. Carvalho, and A. H. Castro Neto, Science **353**, aac9439 (2016).
13. S. C. Dhanabalan, J. S. Ponraj, Z. Guo, S. Li, Q. Bao, and H. Zhang, Adv. Sci. **4**, 1600305 (2017).
14. X. Jiang, S. Liu, W. Liang, S. Luo, Z. He, Y. Ge, H. Wang, R. Cao, F. Zhang, Q. Wen, and J. Li, Laser Photon. Rev. **12**, 1870013 (2018).
15. A. Chernikov, T. C. Berkelbach, H. M. Hill, A. Rigosi, Y. Li, O. B. Aslan, D. R. Reichman, M. S. Hybertsen, and T. F. Heinz, Phys. Rev. Lett. **113**, 076802 (2014).
16. S. Sim, D. Lee, M. Noh, S. Cha, C. H. Soh, J. H. Sung, M. H. Jo, and H. Choi, Nat. Commun. **7**, 13569 (2016).
17. A. Mysyrowicz and D. Hulin, Le Journal de Physique Colloques **49**, C2-175 (1988).
18. F. J. Rodríguez, L. Quiroga, C. Tejedor, M. D. Martín, and L. Viña, AIP Conf. Proc. **893**, 1151 (2007).
19. S. Komineas, S. P. Shipman, and S. Venakides, Phys. D: Nonlinear Phenomena **316**, 43 (2016).
20. M. D. Fraser, Semicond. Sci. Technol. **32**, 093003 (2017).
21. Q. Wang, L. Sun, B. Zhang, C. Chen, X. Shen, and W. Lu, Opt. Express **24**, 7151 (2016).
22. W. Schäfer, K. H. Schuldt, and R. Binder, Phys. Status Solidi **150**, 407 (1988).
23. E. Cancellieri, A. Hayat, A. M. Steinberg, E. Giacobino, and A. Bramati, Phys. Rev. Lett. **112**, 053601 (2014).
24. O. Voronych, A. Buraczewski, M. Matuszewski, and M. Stobińska, Comput. Phys. Commun. **215**, 246 (2017).
25. H. Terças and J. T. Mendonça, Phys. Lett. A **380**, 822 (2016).
26. B. J. Sussman, Am. J. Phys. **79**, 477 (2011).